Motion Control of the Small Fine Arm for the Japanese Experiment Module of the International Space Station

H. Morimoto, Y. Kasama, S. Doi, and Y. Wakabayashi

JEM Project Team
National Space Development Agency of Japan
2-1-1 Sengen, Tsukuba, Ibaraki, Japan 305-8505
morimoto.hitoshi@nasda.go.jp kasama.yuuji@nasda.go.jp
doi.shinobu@nasda.go.jp wakabayashi.yasufumi@nasda.go.jp
Keywords: International Space Station, robotic arm, compliance mode, JEM, JEMRMS

Abstract

The Japanese Experiment Module (JEM) is a part of the International Space Station and has its own robotic arm system, the JEM Remote Manipulator System. It consists of 6-degree-of-freedom robotic arms of two different sizes and their controllers. When the smaller robotic arm is used, the larger robotic arm captures the base of the smaller robotic arm. The smaller robotic arm's main purpose is to replace system payloads to maintain the function of the JEM exposed facility. It has unique features in its motion control, a compliance mode and an active limp mode. When the smaller robotic arm touches the target, a force from the touched target could be transmitted to the arm depending on how it touches the target. While being pushed or pulled by the force, the smaller robotic arm must complete the positioning job with flexibility. The two modes mentioned above play important roles in such a situation. This paper presents the features of the smaller robotic arm's control modes.

1. Introduction

The Japanese Experiment Module (JEM) is a part of the International Space Station and has its own robotic arm system, the JEM Remote Manipulator System (JEMRMS). The JEMRMS consists of a larger robotic arm called the Main Arm (MA: 10m length, 780kg), a smaller robotic arm called the Small Fine Arm (SFA: 2m length, 190kg), and the RMS console (470kg, 2m × 1m × 1m). The RMS console has controllers of the two robotic arms and human-machine interfaces such as a laptop computer, joystick controllers, and TV monitors. Figures 1-1, 1-2, and 1-3 are photos of the Main Arm, the Small Fine Arm, and the RMS console. These are flight models that will be launched in 2004 – 2005, and we are conducting the final test at Tsukuba Space Center in Japan. Figure 1-4 shows artists' concept of the completed JEM. When it is

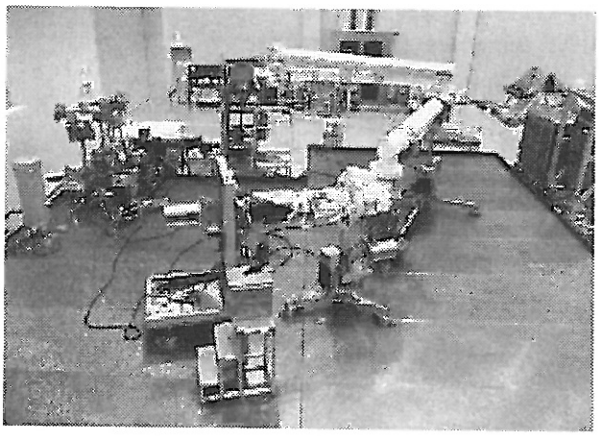

Fig. 1-1 Main Arm (flight model)

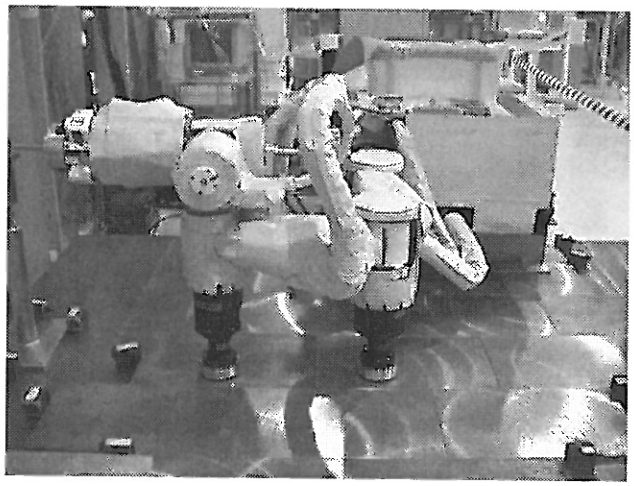

Fig. 1-2 Small Fine Arm (flight model)

completed around 2005, a wide range of space experiments will be conducted. Space robotic arms, including the JEMRMS, are expected to support Extra-vehicle Activities conducted on JEM in order to lighten the load and risks of astronauts. JEM comprises the

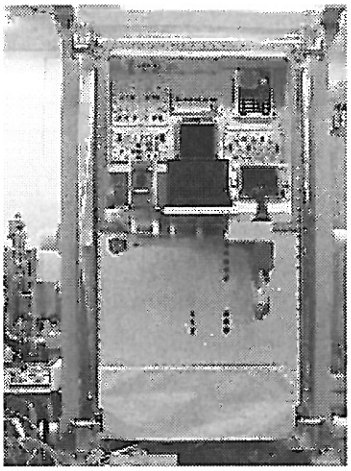

Fig. 1-3 RMS Console (flight model)

Pressurized Module, the Experiment Logistic Module Pressurized Section, the Exposed Facility, the Experiment Logistic Module Exposed Section, and the JEMRMS. The Exposed Facility is a unique platform that

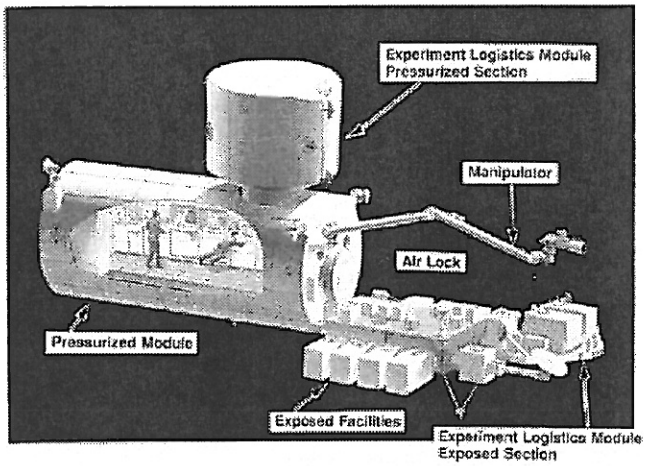

Fig. 1-4 Artist's concept of JEM

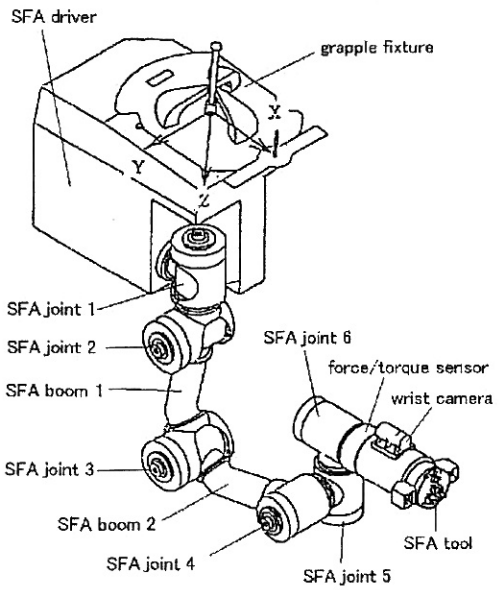

Fig. 1-6 Small Fine Arm

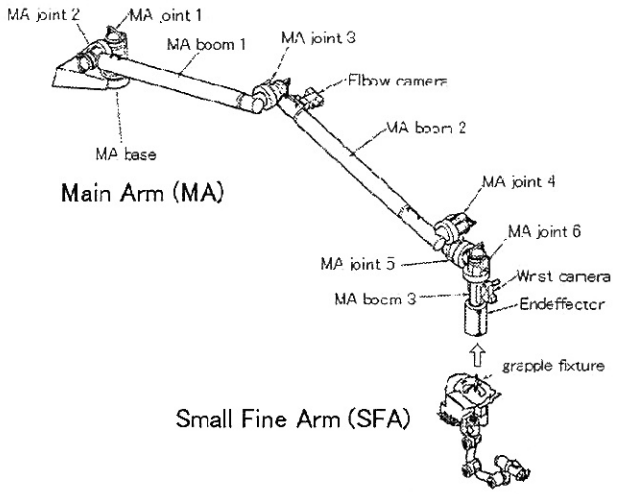

Fig. 1-5 Main Arm and Small Fine Arm

provides a space-exposed environment for up to 10 Standard Experiment Payloads (～500kg, 1m × 1m × 1.85m), which are the Main Arm's payloads. The Experiment Logistic Module Exposed Section is used as a pallet that allows the Main Arm to store up to three Standard Experiment Payloads temporarily. Figure 1-5 shows the two robotic arms. The RMS console includes three computers. One is a modified IBM® Thinkpad® (MMX Pentium® 166MHz) laptop computer that is used as an operation console. The other two are the Management Data Processor and the Arm Control Unit; both are installed inside the RMS console. The console also has two TV monitors to show video images captured by TV cameras installed on the Pressurized Module, the Exposed Facility, the Main Arm and the Small Fine Arm. A Translational Hand Controller and Rotational Hand Controller are installed on the RMS console as a human-machine interface. When a crewmember manipulates the Main Arm or the Small Fine Arm directly in manual mode, the Translational Hand Controller and Rotational Hand Controller work as velocity input devices. The Main Arm is a six-axis, 10m-long robotic arm with an End-Effector, a common device in the International Space Station, at the tip of the arm. The End-Effector is designed to handle objects having a Grapple Fixture, another common interface mating with the End-Effector. The Standard Experiment Payloads and the Experiment Logistic Module Exposed Section have Grapple Fixtures so the Main Arm can handle them. The Small Fine Arm is a six-axis, 2m-long robotic arm as shown in Figs. 1-5

and 1-6. It will be used to replace system payloads (0.6m ×0.4m×0.4m each) on the Exposed Facility. A system payload has a pair of Small Fine Arm Tool Fixtures as an interface with the Small Fine Arm Tool. The Small Fine Arm Tool, a counterpart of the Main Arm's End-Effector, captures the Small Fine Arm Tool. A Grapple Fixture is installed on the Small Fine Arm's driver unit so that the Main Arm's End-Effector can capture it. When the Small Fine Arm is operated, each axis of the Main Arm is servo locked. One of the Small Fine Arm's features is the force moment accommodation modes, the compliance mode and the active limp mode. This paper presents the Small Fine Arm's force moment accommodation modes.

2. Small Fine Arm overview

Table 2-1 shows the Small Fine Arm's specifications.

Length	1.7 m
Weight	190 kg
Maximum payload	300 kg (w/o compliance) 80 kg (w/ compliance)
Positioning accuracy	±10 mm (translational) ±1° (rotational)
Maximum tip velocity	50 mm/s (w/ 0-80kg load) 7.5deg/s (ditto) 25mm/s (w/80-300kg load) 3.7deg/s (ditto)
Emergency stop distance	50 mm
Maximum force Maximum torque	30 N 6 Nm (roll), 4.5 Nm (yaw, pitch)

Table 2-1 Small Fine Arm specifications

The Management Data Processor (MDP) interfaces with the main computers of the JEM Pressurized Module and those of the International Space. Another primary function of the Management Data Processor is to receive commands from the laptop computer called the Remote Laptop Terminal in the RMS console and to forward the commands to the Arm Control Unit (ACU) after verifying their validity. The Arm Control Unit receives rate commands from the Translational Hand Controller and the Rotational Hand Controller when an operator manipulates the Main Arm or the Small Fine Arm in manual mode. When the Arm Control Unit receives a command for the Small Fine Arm from the Management Data Processor, such as "move from the current position to point A," for example, the Arm Control Unit performs the position control calculation that is performed by Joint Electronics Units for the Main Arm. Thus, the Arm Control Unit sends velocity commands to the drive unit of the Small Fine Arm called the Small Fine Arm Electronics instead of position command. When the Arm Control Unit receives a rate command from the Translational Hand Controller and Rotational Hand Controller, it generates a trajectory profile by integrating the rate command. Once a profile is obtained, it is processed as the same way as when the Arm Control Unit receives a command from the Remote Laptop Terminal. MIL-STD-1553B serial buses implement all communication buses mentioned in this section.

3. Motion Control of Small Fine Arm

3.1 Position and velocity loop of Small Fine Arm

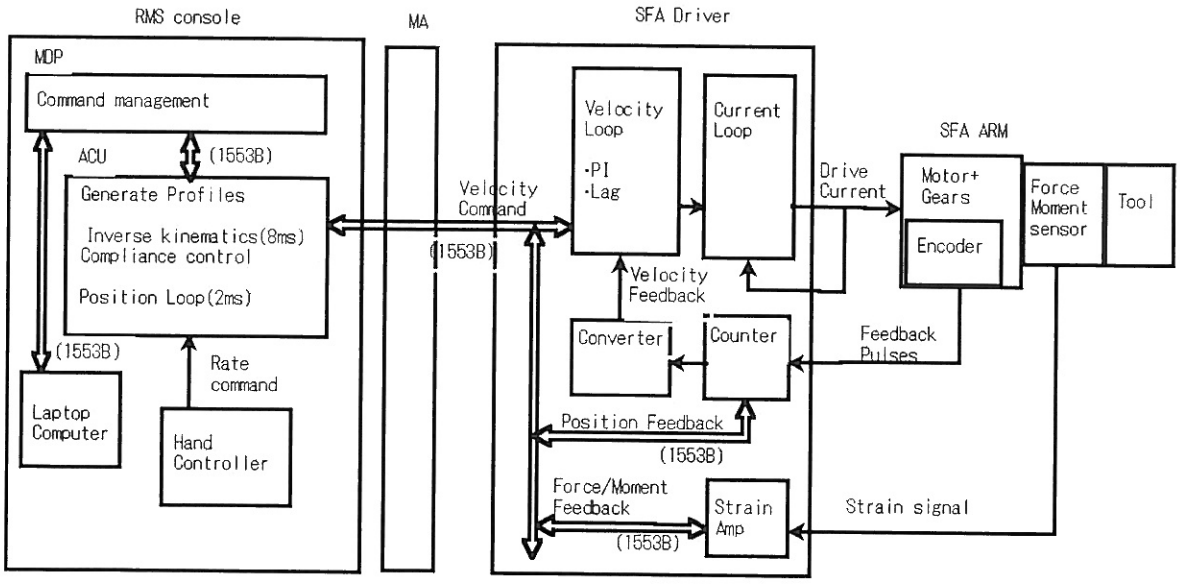

Fig. 3-1 Diagram of Small Fine Arm's control signal transmission

As shown in Fig. 3-1, feedback pulses from the encoder attached to the motor go into a counter in the Small Fine Arm drive unit. The Small Fine Arm drive unit returns the position signal of each axis to the Arm Control Unit, although it receives a velocity command. The Small Fine Arm drive unit also receives strain signals from the force moment sensor of the Small Fine Arm. The signal is amplified by the strain amplifier of the Small Fine Arm drive unit, and its output is forwarded to the Arm Control Unit in order to implement force moment accommodation control. Figure 3-2 illustrates the angular velocity feedback loop of the Small Fine Arm, where each character denotes the following constant or variable.

T: sampling period
Kvi: integral gain of velocity loop
Kvp: proportional gain of velocity loop
b: gain ratio of phase lag compensator
Td: time constant of phase lag compensator
Tvd: time delay due to velocity loop computation
Kip: proportional gain of current loop
La: motor inductance
Ra: motor resistor
Tid: time delay due to current loop computation
Tf: time constant of current filter
Kt: torque constant
Jm: moment inertia of motor
Kf: spring constant of gears
Cf: viscosity friction coefficient of gears
Cfm: viscosity friction coefficient of motor
CfL: viscosity friction coefficient of load
JL: moment inertia of load
TL: load torque
Kef: transmission efficiency coefficient
w*: velocity command
wL: load axis velocity
wm: motor axis velocity

Note that JL, TL, and wL in the diagram should be regarded as already converted from the real values to equivalent ones of the motor axis using the gear ratio. The velocity loop has a PI control path and a phase lag

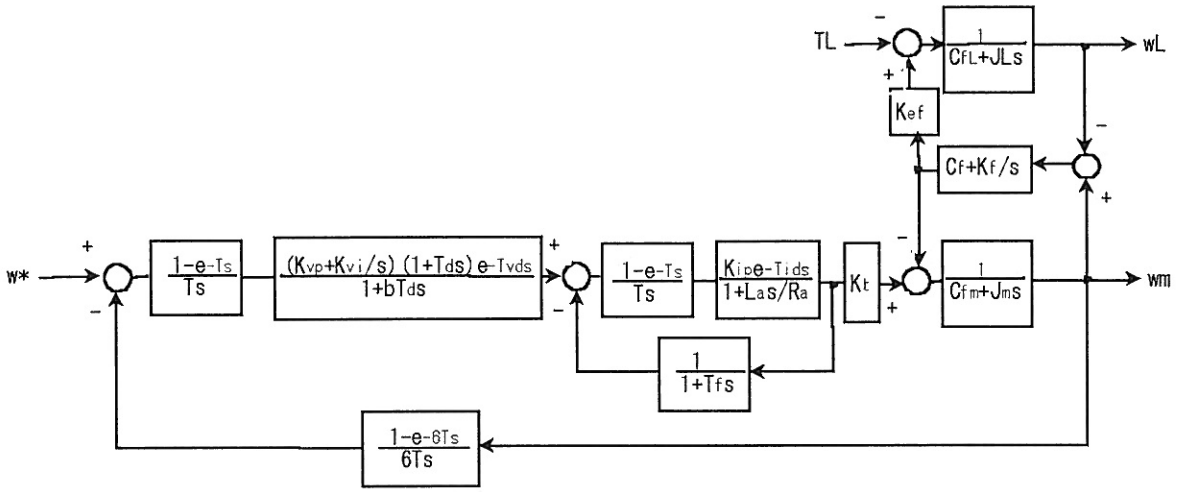

Fig. 3-2 Angular velocity loop of SFA

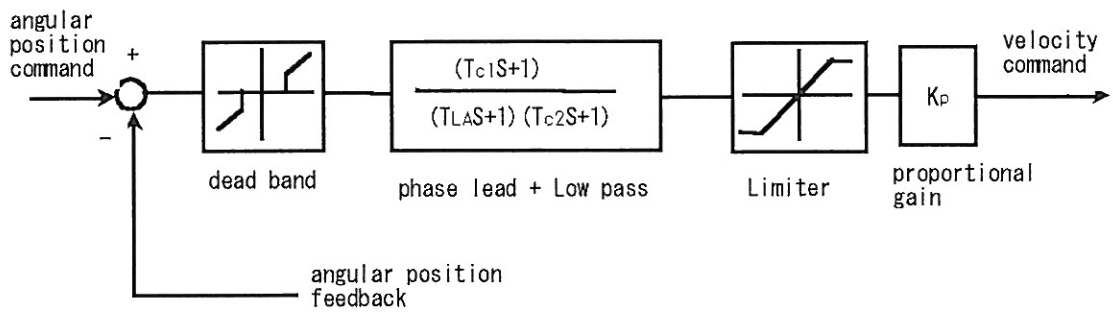

Fig. 3-3 Angular position loop of SFA

compensator. The bandwidth of the loop is ~10 Hz with a 1 ms servo cycle. Figure 3-3 shows the Small Fine Arm's position loop that is implemented by the Arm Control Unit. It works as the P control mode and includes a phase lead compensator with a low-pass filter. The bandwidth of the loop is ~0.5 Hz with an 8 ms servo cycle.

3.2 Force Moment Accommodation Control

3.2.1 Necessity for Compliance mode

The Small Fine Arm compliance mode is required when an operator tries to put a captured system payload in place on the Exposed Facility with a certain positioning error. When a Standard Experiment Payload captured by the Main Arm approaches a ready-to-latch position at one of the ten berthing points of the Exposed Facility, the fingers of a berthing mechanism installed at the berthing point of the Exposed Facility start to capture the Standard Experiment Payload's passive berthing mechanism. While the Standard Experiment Payload is being pulled by the Exposed Facility's berthing mechanism, the Main Arm is kept in the limp mode, in other words, the servo and the mechanical brake are off. Therefore, the Main Arm doesn't have to complete the task by itself; the berthing mechanism does the rest of the job. However, when the Small Fine Arm tries to put a captured system payload in place on the Exposed Facility, there is no berthing mechanism that pulls the payload. Instead, there are only static guiding plates on the Exposed Facility. If the system payload is pushed by the Small Fine Arm, it follows the guide and is placed in the right position. When the Small Fine Arm pushes a system payload against the guide, the compliance mode works so as to reduce the force generated between the payload and the guide. Without the compliance mode, the force could become very large and make positioning harder. The final force is proportional to the number of pulses between the directed position and the current one. A detailed analysis is presented in a later section.

3.2.2 Necessity for Active Limp mode

Another feature of the Small Fine Arm's force moment accommodation control is called "Active Limp Mode". This mode works similarly to the limp mode mentioned in the previous section; the difference is that it is implemented by driving motors. The necessity of the mode can be highlighted by the following example. When the Small Fine Arm captures a system payload, the fingers of the Small Fine Arm Tool open inside the Tool Fixture. As the fingers touch the surface of the Tool Fixture, the force from the surface tries to align the Tool to the Tool Fixture. However, the Tool is not free to move even in the limp mode (servo off and brake off mode) because the back drive torque of the Small Fine Arm can

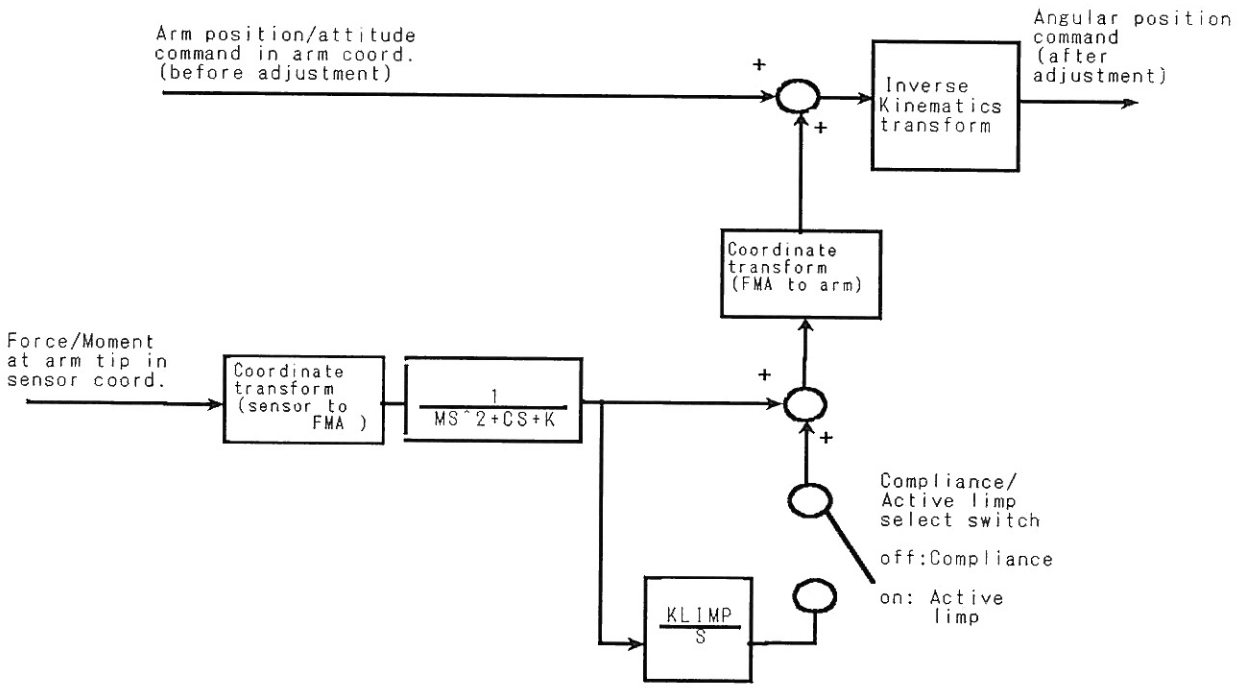

Fig. 3-4 Force Moment Accommodation control

be larger than the torque generated by the fingers' touching the surface of the Tool Fixture. The resistance force and moment that the berthing mechanism must overcome are caused mainly by the back drive torque of the joint's motor/gears and by the harness. Thanks to the planetary gears adopted by the Main Arm, its back drive torque is in a region manageable by the Main Arm's End-Effector. The Small Fine Arm, however, chose Harmonic Drive gears in order to save space, and these introduced rather high back drive torque. This is why the Small Fine Arm's compliance mode is needed.

3.2.3 Features of compliance mode and active limp mode of the Small Fine Arm

Figure 3-4 shows how the compliance mode and active limp mode of the Small Fine Arm work. The force/moment signal at the tip of the Small Fine Arm measured in the sensor coordinate is transmitted to the Arm Control Unit, where the signal is transformed into one in the force-moment accommodation (FMA) coordinate. This coordinate can be chosen arbitrarily. For instance, it could be aligned to the fixed direction of the Tool Fixture, which the fingers of the Tool follow. One can even apply the FMA controls to only one of the three axes. The force/moment signal then applies to a virtual mass-damping-spring system. By applying $1/(Ms^2+Cs+K)$ to the force/moment signal where M, C, and K are a virtual mass, a damping coefficient, and a spring constant, one can obtain a virtual displacement in the FMA coordinate as a response of the virtual system to the measured force/moment. In the compliance mode, this virtual displacement in the FMA coordinate is transformed to the arm coordinate so that it is added to the arm position/attitude command of the same coordinate. This summing lightens the force/moment generated between the touched object and the arm because the virtual displacement is in the direction of the force. The corrected position/attitude command is next converted to angular displacement of each axis by an inverse kinematics calculation. For the active limp mode, the integral of the virtual displacement in the FMA coordinate is also summed to the virtual displacement. The sum of the two quantities is next transformed to the arm coordinate, and the rest process is the same as for the compliance mode. The effect of adding the integral can be explained as follows. After a certain response of the virtual mass-damping-spring system to the applied force/moment, any remaining force/moment signal from the force moment sensor is accumulated by the integral term, and thus, the term keeps on reducing the pulse difference between the commanded position and the current one, which decreases the amount of the force/moment generated by the motor axis. Eventually, the process of reducing the pulse difference stops when no force/moment remains. In the compliance mode, there is a certain point where the force/moment balances the one generated by the motor axis that corresponds to some pulse difference. Therefore, if the applied force is released, (i.e., the constraint is removed), the arm will go to the commanded position in the compliance mode, but will stay there in the active limp mode. This is the reason that the mode is called "active limp." A quantitative discussion is given in the following section.

3.2.4 Analysis of Compliance mode

Consider a simplified case in which the arm coordinate is chosen as the FMA coordinate. Furthermore, assume the arm coordinate is aligned to the force/moment sensor coordinate. Thus, the laborious coordinate transforms don't need to be done. We also assume that the direction in which the FMA control is applied is limited to only one of the three axes, thus the problem becomes one-dimensional. Another assumption here is that the arm is constrained to a fixed Tool Fixture in space. The arm pushes or pulls the fixture, but, because it is fixed in space, the arm doesn't move. Therefore, the complex nonlinear dynamics of the arm don't have to be considered. The motor dynamics in the velocity loop is also omitted from consideration because the arm stays still. Based on these facts, the block diagram that represents the

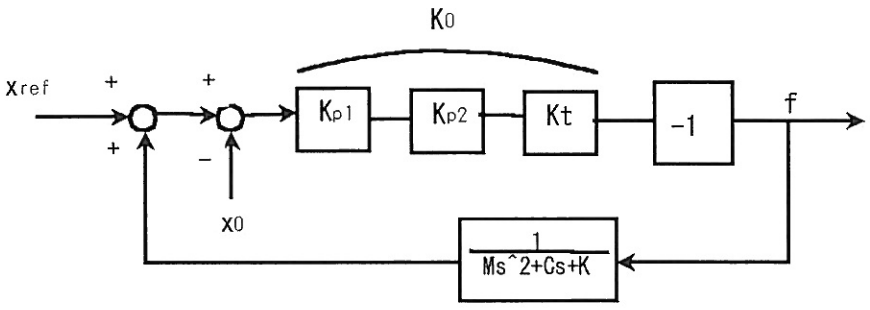

Fig. 3-5 Diagram of x_{ref} vs f in compliance mode

relationship between the commanded position x_{ref} and the resistant force/moment f caused by the motor axis is shown in Fig. 3-5.

x_0 is the constrained arm position that is therefore constant here. K_{p1} denotes the product of the proportional gain K_p in the position loop and the gain of the phase lead filter in Fig. 3-3. K_{p2} represents the product of the proportional gain K_{vp} and other proportional elements before K_t included in the velocity loop in Fig. 3-2. The negative sign after K_t in Fig. 3-5 shows that f denotes a force/moment applied from the touched object to the arm. Let K_0 be the product of K_{p1}, K_{p2}, and K_t to simplify notation. The transfer function between $(x_{ref} - x_0)$ and f, $G_{comp}(s)$ is then calculated as follows.

$$G_{comp}(s) = -\frac{K_0(Ms^2 + Cs + K)}{Ms^2 + Cs + K + K_0} \quad (1)$$

Suppose the input command $x_{ref} - x_0$ is written as Eq. (2),

$x_{ref} - x_0 = mt$ (m:constant) $(t<t_1)$

$x_{ref} - x_0 = d$ (constant) $(t>=t_1)$ (2)

Substituting designed values for the constants in eqs. (1) and (2), f (t) is obtained as illustrated in Fig. 3-6. Let X(s) be the Laplace transform of (2), then because all poles of $s \cdot G_{comp}(s) \cdot X(s)$ lie in the left half plane, $\lim_{t\to\infty} f(t)$ exists as observed in Fig. 3-6. Thus, the steady-state value of f (t) is evaluated as follows. Let f_{ss} denote the steady-state value of f (t).

$$f_{ss} = \lim_{s\to 0} s \cdot G_{comp}(s) \cdot X(s) = -\frac{dK_0 K}{K + K_0} \quad (3)$$

where d is defined as $d = mt_1$, i.e., the virtual distance between the commanded position and the current position after $t = t_1$.

In order to obtain engineering data for the Small Fine Arm's design, on-orbit robotic experiments using a robotic arm that had similar features as the Small Fine Arm were conducted in 1997 and 1998. The experiment in 1997 was called Manipulator Flight Demonstration (MFD), and was conducted in the cargo bay of the Space Shuttle on the orbit. In 1998 a space robotic arm experiment that was installed on NASDA's Engineering Test Satellite VII was

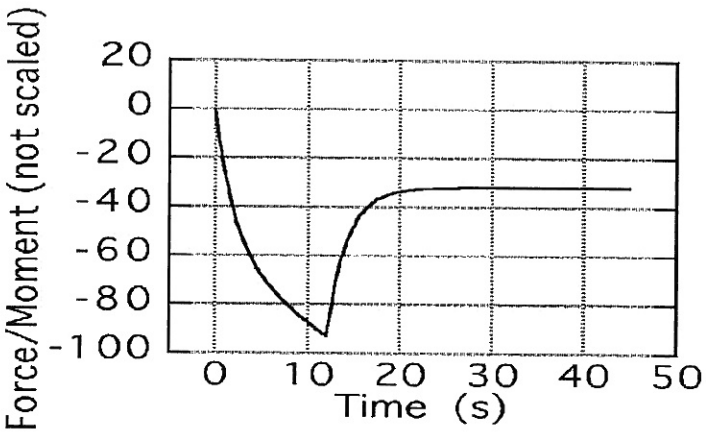

Fig. 3-6 Force/moment in compliance mode (simulation)

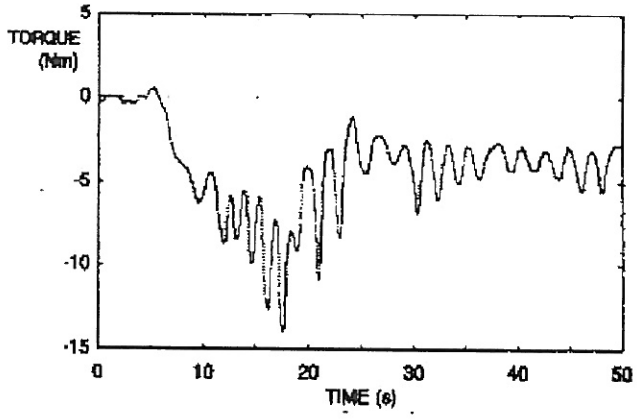

Fig. 3-7 Force/moment in compliance mode (Test data in the MFD experiment)

conducted. For comparison between the simulation and the reality, test data of the MFD are shown in the Fig. 3-7.

In the experiment, ramp commands for rotation of the tip were sent, while the arm was constrained to a fixed point. Figure 3-7 shows the measured torque in such conditions in the compliance mode. Although the damping factor set in the MFD experiment was smaller than that of the simulation in Fig. 3-6, the oscillation observed in the Fig. 3-7 may have other causes than the parameter setting of M, C, and K in the experiment.

3.2.5 Analysis of active limp mode

With the same assumptions as in the compliance mode, the block diagram that represents the relationship between the commanded position x_{ref} and the resisting force/moment f caused by the motor axis is illustrated in Fig. 3-8. The notation in Fig. 3-8 is the same as in Fig. 3-5. In addition, K_{LIMP} is introduced in Fig. 3-8 and is a constant for the integral term in the loop. The transfer function between $(x_{ref} - x_0)$ and f, $G_{ALIMP}(s)$, is calculated in the same way as $G_{comp}(s)$. The result is shown below.

$$G_{ALIMP}(s) = -\frac{sK_0(Ms^2+Cs+K)}{Ms^3+Cs^2+(K+K_0)s+K_0K_{LIMP}} \quad (4)$$

We consider an output f (t) to the same input expressed by eq. (2).

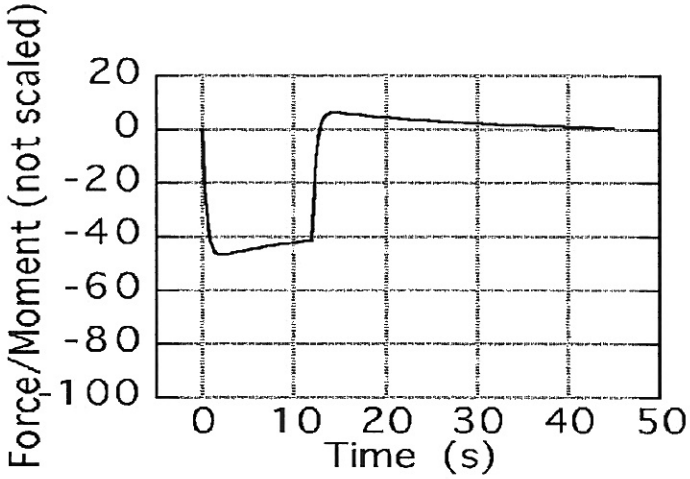

Fig. 3-9 Force/moment in active limp mode (simulation)

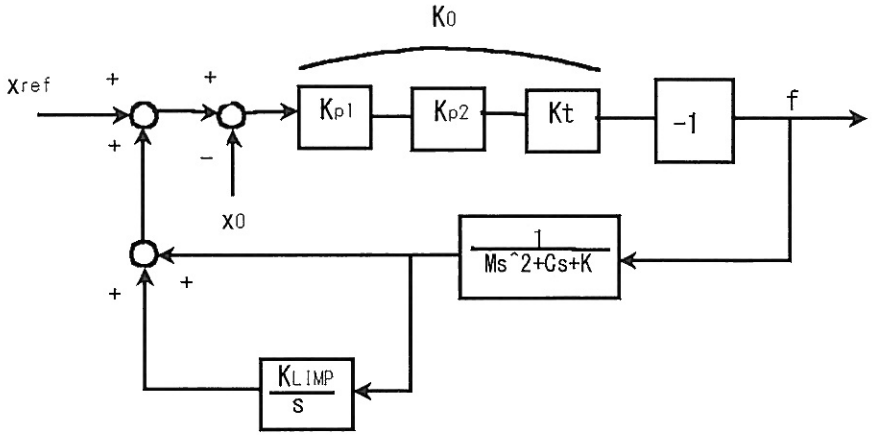

Fig. 3-8 Diagram of x_{ref} vs f in active limp mode

Substituting designed values for the constants in eqs. (2) and (4), f (t) is obtained as illustrated in Fig. 3-9. Because all poles of $s \cdot G_{ALIMP}(s) \cdot X(s)$ lie in the left half plane, $\lim_{t\to\infty} f(t)$ exists as observed in Fig. 3-9. Let f_{ss} denote the steady-state value of f (t).

$$f_{ss} = \lim_{s\to 0} s \cdot G_{ALIMP}(s) \cdot X(s) = 0 \quad (5)$$

As in the previous section, test data of the MFD is shown in the Fig. 3-10 for comparison with simulation. Figure 3-10 shows the measured torque in the active limp mode for the same conditions as in Fig. 3-7. Note again that oscillation observed in figure 3-10 may have other reasons than the parameter set M, C, K, and K_{LIMP} chosen in the MFD experiment.

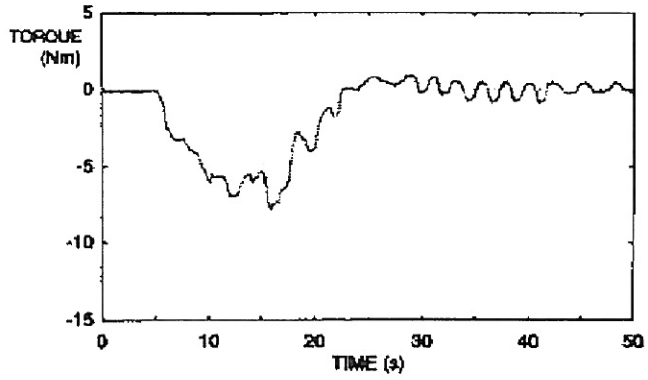

Fig. 3-10 Force/moment in active limp mode (Test data in the MFD experiment)

4. Conclusion

The purpose and implementation of the force moment accommodation control of the Small Fine Arm were presented. A simple simulation model was found useful to predict experiment results. Both in the compliance mode and in the active limp mode, the force/moment simulation curve shows no oscillation unlike the measured ones in the MFD experiment. The reasons for the oscillation is not identified yet. A thorough test using the Small Fine Arm flight model will soon start this year. The test is expected to clarify the difference observed here between the simulation and the MFD experiment data.

References

[1] Nishida, S. et al., ``Engineering Test Satellite VII Robot Experiment System,'' *Journal of the Robotics Society of Japan*, Vol. 17, No. 8, pp. 1062-1066, 1999. (In Japanese)

[2] Nagatomo, M. et al., "Development and Operation of Manipulator Flight Demonstration System," *Proceedings of Manipulator Flight Demonstration Symposium*, pp. 41-51, March 1998. (In Japanese)

[3] Doi, S. et al., "Control Aspect of Japanese Experiment Module Remote Manipulator System," IFAC conference paper at Telematics Applications in Automation and Robotics, July 2001. (To be appeared)

[4] Oda, M. et al., "Space robot experiments on NASDA's ETS-VII satellite," *Proceedings of The 29th International Symposium on Robotics*, April 1998, Birmingham, England

[5] Nagatomo, M. et al., "Results of the On-Orbit Manipulator Flight Demonstration (MFD)," Proceedings of The 21st International Symposium on Space Technology and Science, May 1998, Omiya, Japan